Electronic conduction in polyaniline-polyethylene oxide and polyaniline-Nafion blends: Relation to morphology and protonation level

B. Sixou and J. P. Travers*
Laboratoire de Physique des Métaux synthétiques, Unité Mixte de Recherche 585, Département de Recherche Fondamentale sur la Matière, Condensée/Commissariat à l'Energie Atomique, 17 rue des Martyrs, 38054 Grenoble Cedex 9, France

C. Barthet and M. Guglielmi
Laboratoire de Physico-Chimie Moléculaire, Unité Mixte de Recherche 585, Département de Recherche Fondamentale sur la Matière, Condensée/Commissariat à l'Energie Atomique, 17 rue des Martyrs, 38054 Grenoble Cedex 9, France
(Received 22 November 1996)

We present a comprehensive study of the transport properties in polyaniline-Nafion and polyaniline-polyethylene oxide, lithium trifluoromethane sulfonimide complex blends, together with a careful characterization of the morphology and the polyaniline protonation level. They include conductivity measurements as a function of both the polyaniline content of the blends and the temperature for a given composition. We show that percolation theory can account for the data provided that hopping and tunneling are taken into account. Moreover, in the polyaniline-Nafion blends, the variation of the polyaniline protonation level with the blend composition appears as a crucial parameter. The leading conduction mechanism is shown to be a hopping process between highly conducting polyaniline grains, the parameters of which are determined by the blend composition, and the protonation level. [S0163-1829(97)07031-8]

I. INTRODUCTION

Electrical conduction in insulator-conducting composites, including electronically conducting polymers, has been the subject of many experimental and theoretical studies.[1–11] From a technological point of view, these materials are very interesting because they combine electronic conduction and the desired mechanical properties of the insulating matrix. Recently, a new class of homogeneous, stable and processible polymer blends based upon polyaniline (PANI) has been synthesized. In these materials, the threshold for the onset of the electrical conductivity can be reduced to very low volume fractions of PANI and the increase of the conductivity above the threshold is very smooth. Therefore, conducting polyblends can be obtained with controlled levels of electrical conductivity, while retaining the mechanical properties of the matrix polymer.[8–11]

Among these materials, the blends in which polyaniline is associated with an ionic matrix are of particular interest. First, the doping/undoping process kinetics of a massive electrode are strongly improved by the greater proximity of the required ions to the polyaniline chains in the case of such blends, as compared with that case of a pure PANI electrode.[12] This property is very attractive for applications using the electrochemical properties of an electronically conducting polymer (ECP), such as energy storage devices.

Besides, from a fundamental point of view, the study of the electrical conductivity of these composites can shed light on the particular nature of the percolation phenomena in such types of blends, as well as on the role played by the dopant in the conduction mechanisms of the pure material.[13,14] New information is expected (i) on the changes in the classical percolation threshold and exponent resulting from hopping and tunneling processes, (ii) on the influence of a correlation between the composition and the protonation level on the theoretical scaling laws, as well as on the ability of the dopant to act as a tunneling bridge between neighboring chains.

In this paper, we are interested in the transport properties of two such blends based on polyaniline: polyaniline in polyethylene oxide, lithium trifluoromethane sulfonimide complex (PANI/PEO), and Nafion-doped polyaniline (PANI/NAFION). Nafion is a registered trademark for an ionomer made up of a hydrophobic perfluorinated skeleton on which are grafted lateral chains terminated by sulfonate groups.[13,14] The PANI/PEO mixture has been mainly used in solid state batteries,[15] while the PANI/NAFION one has been studied in batteries,[15,16] electrocatalysis,[17] sensors,[18] and electrochromic devices.[19] We present here a study of the electronic transport processes in these blends, which has been carried out in close relationship with both the distribution of the PANI phase in the two different matrices and the organization of the doped and undoped parts of the ECP in the blends.

We paid special attention to the blend preparation in order to obtain molecular scale mixtures and to minimize the heterogeneities during the protonation process. This was achieved using a method based upon the emeraldine base (EB) property to dissolve in polar solvents[20] and on its liquid phase protonation.[21] Well-characterized samples of these blends with different compositions have been studied with a particular look at the morphology and the PANI protonation levels. We have measured the variation of room temperature conductivity as a function of the PANI composition, as well as the temperature dependence of the conductivity for different compositions.

We show that PANI/PEO blends behave similarly to numerous polymer mixtures already reported in the literature and can be approximately described by percolation models. The observed deviations from the basic theory may be attrib-

uted to doping heterogeneities and to hopping and tunneling conduction processes.

The PANI/NAFION displays a more original behavior, which comes from the correlation between the doping level of polyaniline and the blend composition. From the thermal variation of the conductivity it appears that hopping processes between conducting clusters govern the transport mechanisms. Special attention is paid to a particular PANI/NAFION blend, containing a low volume fraction of highly doped polyaniline, in which the conductivity displays a specific temperature dependence that is ascribed to a disconnected pathway between very large conducting grains.

II. EXPERIMENTAL SECTION

A. Sample preparation

The PANI/PEO preparation consists of the dissolution in *N*-methyl-2-pyrrolidinone (NMP) at 40–50 °C of varying proportions of EB, PEO, and lithium trifluoromethane sulfonimide (LiTFSI). The protonation of EB is achieved by addition of trifluoromethane sulfonimide acid (HTFSI) in the NMP solution, in suitable proportions to obtain a 50% doping of the aniline units by the TFSI anions. Solutions containing 20, 40, 60, 70, 90, and 100% weight fraction of PANI have been prepared.[22] These fractions correspond to the ratio of the mass of emeraldine (EB) to that of all the components (EB, PEO, and LiTFSI) of the mixture. The molar ratio of PEO to LiTFSI is kept constant and corresponds to 20 mol of oxygen for 1 mol of lithium.[21] Films are obtained after heating the solutions deposited on a flat surface from 60 °C to 120 °C under vacuum, with an increase of 5 °C every hour. The volume fractions f of PANI in the films, 14%, 31%, 50%, 61%, 86%, and 100%, are calculated taking the $\text{density}_{\text{PANI}}=1.4$ (Ref. 20) and $\text{density}_{\text{PEO}}=0.95$.[23]

Stable solutions of Nafion-doped polyaniline have been obtained and described elsewhere.[13,24] Various quantities of the acid form of Nafion are added to a solution of emeraldine base in NMP. The protonation of the emeraldine base by the sulfonic groups of Nafion is shown by the change in color from blue to dark green. The PANI/NAFION solutions contain 7, 15, 20, and 30% weight of PANI relative to the mass of the two polymers. The PANI/NAFION films are prepared in the same manner as the PANI/PEO films. The volume fractions f of PANI in the films, 10%, 20%, 26%, and 38%, are calculated taking the $\text{density}_{\text{NAFION}}=2$.[21] More details are given in Refs. 21 and 22 for the preparation of PANI/NAFION and PANI/PEO, respectively.

B. Characterization methods

The morphology of the PANI/PEO has been observed with a scanning electron microscope (SEM) model Jeol 840. Transmission electron microscopy (TEM) observations have been made on the PANI/NAFION with a Philips Model CM 120 microscope on ultramicrotomed sections of dry films labeled by exposure to OsO_4 vapors.

UV-visible near-infrared spectra of the 100-μm-thick films were recorded in the range 250–1000 nm with a Perkin Elmer spectrophotometer Lambda 9.

C. Electronic conductivity measurements

The room-temperature conductivity was measured by the collinear four-probe method. Several samples of each composition were used in order to evaluate the mean value of the conductivity and standard deviations. As concerns the temperature dependence of the conductivity, a conventional four-probe method was applied by mechanically pressing films of typical size $8\times5\times0.05$ mm^3, on four parallel gold wires.

The dc current was provided by a Keithley 220 current source and two Keithley 617 programmable electrometers with an input impedance of 10^{14} Ω were used to measure the voltage drop between the inner contacts. The linearity of the voltage versus current characteristics was systematically checked on a one order of magnitude current range. Possible thermoelectric effects were excluded by measurements in both current senses.

The measurements were performed in an Oxford Instrument cryostat in the range 15–300 K. The cell was placed into a closed chamber filled with a low pressure of He as an exchange gas. The maximum average power dissipated in the sample from the generator was 5 μW. The sample temperature was measured using a calibrated platinum resistor in the range 300–40 K or a calibrated carbon glass resistor in the range 40–15 K.

III. RESULTS AND DISCUSSION

A. Morphologies and protonation levels

1. PANI/PEO

When HTFSI is added to the solution of EB, PEO, and LiTFSI, as mentioned in the preparation above, the films prepared from that mixture exhibit a continuous background as shown by SEM micrographs and thus a homogeneous and compact structure at the micrometer scale whatever the composition [Fig. 1(a)]. On the contrary, the micrographs of films obtained from a mixture of EB, PEO, and LiTFSI only show a strong porosity, which indicates segregation of the two polymers [Fig. 1(b)]. Hence, the HTFSI protonation of the emeraldine base in the solution leads to a dense material and we expect a homogeneous distribution of the ECP in the polyether matrix. The analysis of this material by Fourier-transform infrared (FT-IR) spectroscopy has shown that the entanglement of the PEO and the PANI chains hinders the return of the PEO to its more stable helicoidal form.[21] Besides, we have noticed that the PEO moiety of the material is not soluble in the classical solvents of PEO. The HTFSI-doped PANI interacts strongly with the polyether complex. Thus, in order to synthesize blends, the higher the doping level of the PANI chains, the greater the affinity between the two polymers and the more homogeneous the polymer mixture.

The protonation level of PANI, defined as the proportion of counterions per aniline ring has been deduced from x-ray photoelectron spectroscopy (XPS) measurements.[21,22] It must be emphasized that protonation in pure EB leads to the formation of 50% protonated conducting islands, which coexist with unprotonated insulating regions and thus the maximum protonation level is actually 50%. From the deconvolution of the N 1*s* core-level spectra into contributions corresponding

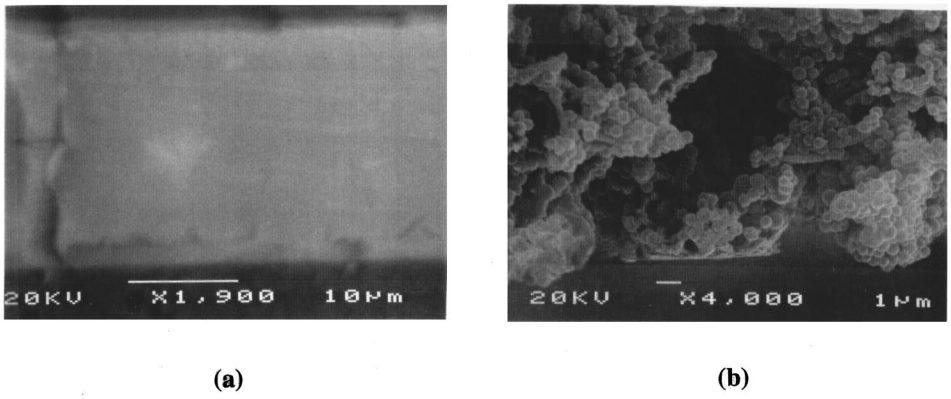

FIG. 1. SEM micrographs of PANI/PEO films (a) issued from the HTFSI protonation of PB in solution in NMP; (b) issued from a mixture of EB, PEO, and LiTFSI only.

to different species of nitrogen atoms, the protonation level is obtained as the sum of the contributions associated with positively charged species coming from the protonation of amine (—NH—) and imine (—N═) nitrogen species of EB chains. The results are given in Table I for blends with 31 and 61 vol% of PANI. The protonation level is about 43.5 ±1.0%, whatever the proportion of the ECP in the mixture, which is typical of a fully protonated conventional PANI sample.

Figure 2 shows the characteristic UV-visible near-infrared spectrum of PANI/PEO films with 31 and 61 vol% of PANI. The electronic structure does not vary with the PANI volume content, which means a constant level of PANI protonation with composition as shown by XPS measurements. Two peaks attributed to the protonated state are situated near 400 and 870–890 nm (Ref. 25) and a shoulder, typical of the emeraldine base form, is visible at 620–630 nm.[26] The coexistence of the peaks close to 640 and 900 nm, characteristic of the undoped and doped states, respectively, shows the various states of protonation of the ECP chains. The above results give support to the idea that the microscopic organization of the blend remains the same whatever the composition.

2. PANI/NAFION

In the blends with 20 and 26 vol% of PANI, TEM micrographs show large islands composed of 20–30 nm interconnected PANI areas embedded in the NAFION net[13] (Fig. 3). For a low PANI content (10%), we observe similar islands separated by a larger ionomer phase. This suggests that the ionic interactions between the sulfonate groups of NAFION and the protonated nitrogen atoms of the PANI chains govern the organization of the ECP and shows that the distribution of the polymers does not vary much with the composition of the films in the explored composition range.

Elemental analyses have shown that the average doping level δ, reported in Table II, varies from 0.19 to 0.4 depending on the ratio of the number of sulfonate groups to the number of aniline units:[24] in the blend with 38 vol% of PANI, nearly all the sulfonate groups participate in the doping process, while in the blend with 10 vol% of PANI, they are in strong excess. The fact that all the sulfonate groups act as doping agents until their concentration becomes in excess is a strong indication in favor of a good dispersion of the ECP in the ionomer.

Figure 4 shows the characteristic UV-visible spectra of PANI/NAFION films as a function of the PANI volume content. The two peaks, situated at 420–450 and 860–960 nm,

TABLE I. Protonation level of PANI in different PANI/PEO films as determined by the deconvolution of the N 1*s* core-level spectra. The uncertainty on the binding energies is of ±0.1 eV.

PANI volume content, f(%)	31	61
Unprotonated imine (—NH—) Nitrogen (%)[a]	22.3	17.6
Unprotonated amine (—N═) Nitrogen (%)[b]	34.6	38.8
Protonation level (%)[c]	43.1	43.6

[a]Component at 398.8 eV.
[b]Component at 399.8 eV.
[c]Sum of the proportions of the radical cation, protonated imine, and protonated amine forms of PANI (components at 400.7 and 401.8 eV).

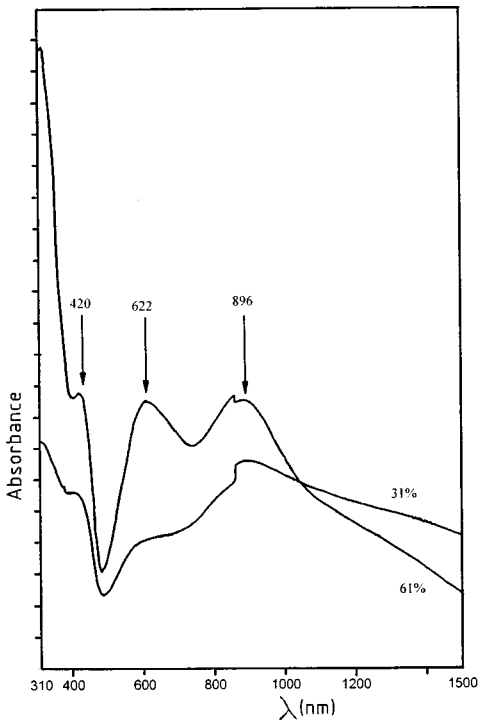

FIG. 2. UV-visible near-ir spectra of PANI/PEO films for different PANI volume contents. The discontinuity observed around 850 nm comes from a change of the spectrophotometer setting.

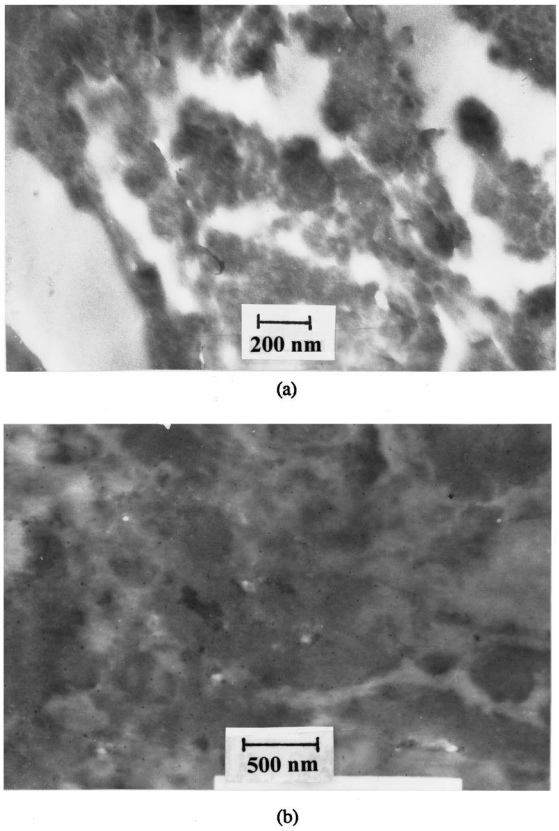

FIG. 3. TEM micrographs of PANI/NAFION films with 20 or 26 vol% of PANI (a) before and (b) after labeling the NAFION phase with OsO_4 vapors.

result from the formation of a polaronic network.[25] A shoulder is also observed at 620–660 nm,[26] which increases in intensity with the rise in the PANI concentration. This increase indicates, as expected, a growing undoped phase that coexists with a highly doped phase in the films. When the PANI volume fraction reaches 38%, one could expect a segregation of the PANI phase due to a lack of electrostatic interactions between the sulfonate groups of the ionomer and the PANI chains in excess.

The above characterization of the materials gives information about the distribution of the PANI in the two different matrices. Creating interactions between the ECP and an ionic polymer matrix by protonation of the emeraldine base seems an interesting way to obtain PANI-based blends in spite of the steric effects that can limit the process. Both mixtures appear as very disordered materials including doping heterogeneities of the ECP, and we expect that such a structure will determine the transport properties. Then, one can see that, while the PANI/PEO films have a high but constant level of protonation, the specificity of the PANI/NAFION ones lies in the correlation between the PANI doping level and the composition. A particular evolution of transport properties with the PANI content is thus expected in the PANI/NAFION blend.

TABLE II. Protonation levels of PANI determined by elemental analysis in the PANI/NAFION films of varying compositions.

PANI volume content f (%)[a]	SO_3^-/aniline[b]	Average doping level[c]
10	1.1	0.4
20	0.5	0.27
26	0.33	0.26
38	0.2	0.19

[a]PANI volume fractions calculated from the ratio of the polyemeraldine volume to the volume of all the components (PB, PEO, and LiTFSI) in the mixture.

[b]Calculated from the ratio of the number of sulfonate units to the number of aniline units in the mixture.

[c]Average doping level measured by elemental analysis (Ref. 21).

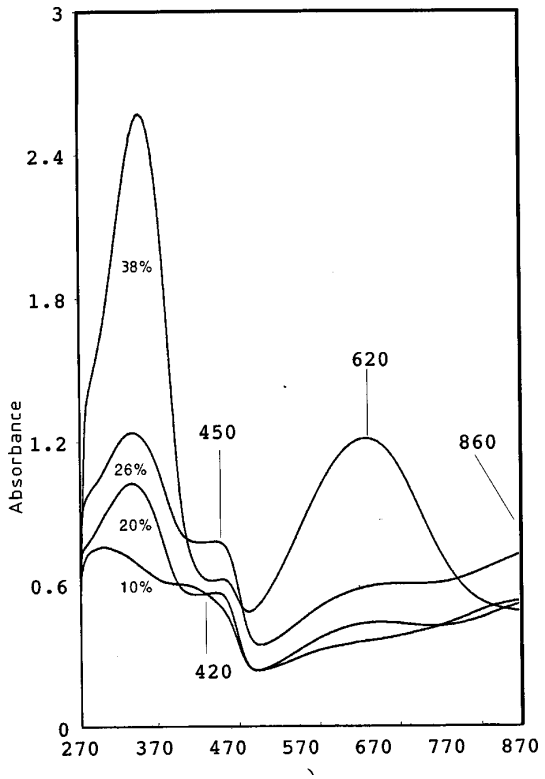

FIG. 4. UV-visible spectra of PANI/NAFION films for different PANI volume contents.

B. Electronic conduction

1. PANI/POE

The room-temperature dc conductivity shows a continuous increase as a function of the volume content of polyaniline, f, as can be seen in Fig. 5. From different samples with the same polyaniline content, we have estimated the relative uncertainty on the conductivity values to be about 15%. To test the predictions of the percolation theory, the data have been fitted with the scaling law:

$$\sigma(f) = C|f - f_c|^t, \tag{1}$$

where f_c is the percolation threshold, C a constant, and t the critical exponent.[27] One can see in Fig. 5 that the agreement between the data and this theoretical law is qualitatively good on the whole range of composition while it is expected to be valid only near the percolation threshold. Yet, it must be pointed out that the small amount of data and the rather large conductivity uncertainties prevent any accurate deter-

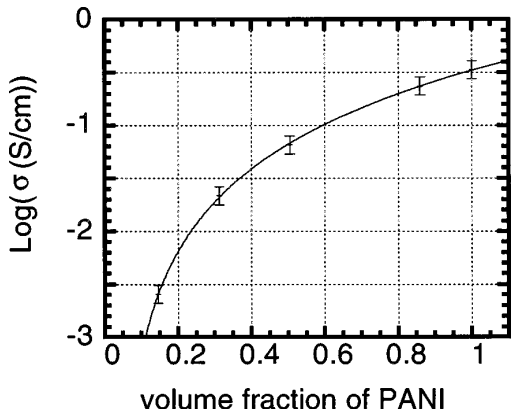

FIG. 5. Variation of the decimal logarithm of the room-temperature conductivity of the PANI/PEO blends as a function of the volume content of PANI. (---): best fit obtained with Eq. (1).

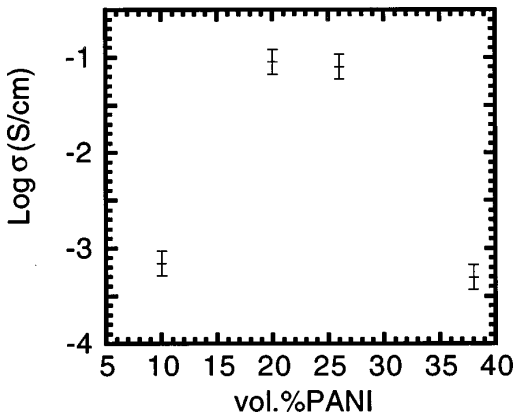

FIG. 7. Variation of the decimal logarithm of the room-temperature conductivity of the PANI/NAFION blends as a function of the PANI volume content.

mination of both the percolation threshold and the critical exponent and thus of the critical region. In addition, on a fundamental point of view, very little is actually known about the extent of this region and, experimentally, the validity of the scaling law (1) on the entire concentration range has already been found in carbon black composites.[10,28] When the fit is restricted to the data near the percolation threshold and when the conductivity uncertainties are taken into account, approximate values for t and f_c, $2.2<t<2.5$ and $3.5\%<f_c<5.5\%$ can be determined. Despite this uncertainty, t appears to be quite different from its universal theoretical value[27] $t=2$.

We have tried to fit the thermal evolution of the conductivity with a law characteristic of a hopping-type mechanism:

$$\sigma=\sigma_0\exp[-(T_0/T)^{\alpha}], \tag{2a}$$

with σ_0 a constant. As shown in Fig. 6, the exponent $\alpha=1/2$ leads to good fits for the whole data set. The experimental data and thus the variation of the conductivity are rather well described by the following law:

$$\sigma=\sigma_0\exp[-(T_0/T)^{1/2}]. \tag{2b}$$

Such a temperature dependence has been observed in bulk HCl-doped polyaniline and many PANI blends obey the same relation.[29] The parameter T_0, which corresponds to the slope of the former curves, decreases with increasing volume contents of PANI from $T_0=5.5\times10^4$ K (13,6 vol% PANI) to $T_0=1\times10^4$ K (100 vol% PANI).

2. PANI/NAFION

The room-temperature conductivity is reported in Fig. 7 in a logarithmic scale as a function of the volume content of PANI. The relative uncertainty on the data was estimated as 30%. The conductivity displays a maximum, $\sigma\approx0.1$ Siemens/cm (S/cm), for the blends with 20–26 vol% of PANI.

As concerns the samples with 20, 26, and 38 PANI vol%, the best fit to the $\sigma(T)$ data was achieved with $\alpha=1/2$ [Eq. (2b)] as shown in Fig. 8. The variation of T_0 as a function of the content of conducting polymer is reversed as compared to PANI/POE. The blend with 38 vol% of PANI has a stronger temperature dependence and a higher T_0 value ($T_0=43\,700$ K) than the samples with 26 or 20% PANI ($T_0=29\,600$ and 21 900 K, respectively).

As shown in Fig. 9, the same law does not fit the data in the case of the blend with 10 vol% of PANI, neither does any law of the type described by Eq. (2a). On the other hand, the fluctuation-induced tunneling (FIT) model of Sheng,[30] dedicated to the case of large conducting grains accounts quite well for the data. In the framework of this model, the conductivity is given by

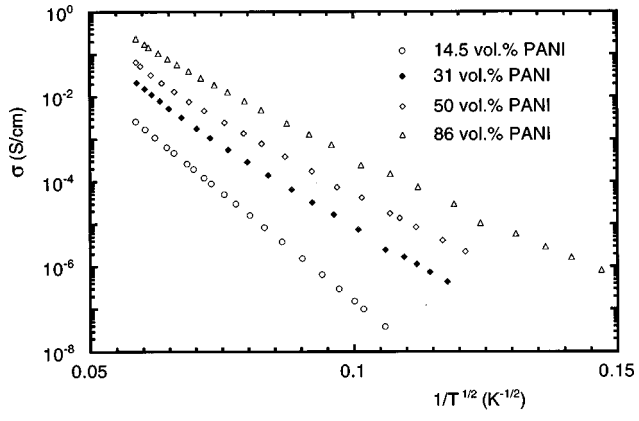

FIG. 6. Logarithmic plots of σ vs $1/\sqrt{T}$ for the PANI/POE blends.

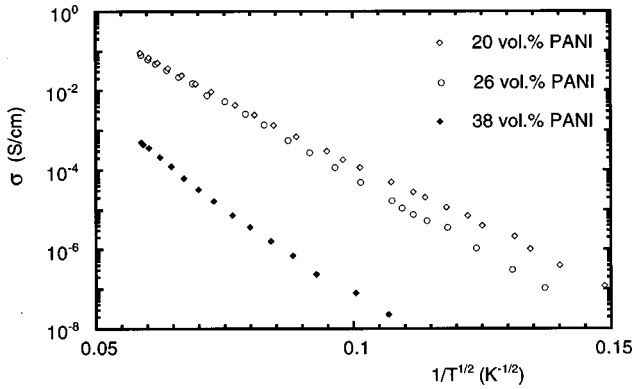

FIG. 8. Logarithmic plots of σ vs $1/\sqrt{T}$ for the PANI/NAFION blends with 20, 26, and 38 vol% of PANI.

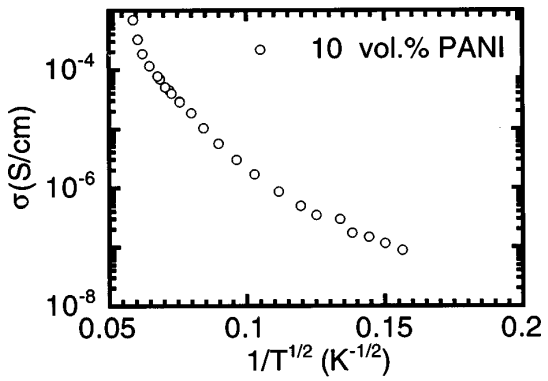

FIG. 9. Logarithmic plot of σ vs $1/\sqrt{T}$ for the PANI/NAFION blend with 10 vol% of PANI.

$$\sigma = \sigma_0 \exp\left(-\frac{T_1}{T+T_0}\right), \tag{3}$$

where σ_0, T_1, and T_0 are constants. As shown in Fig. 10, good agreement is obtained on a wide temperature range, using $T_1 = 6300$ K, $T_0 = 280$ K, and $\sigma_0 = 32$ S/cm.

C. Discussion

1. PANI/PEO

In the framework of percolation theory, the geometrical aspect of the conducting network, and its intrinsic conductivity appear as separate variables [Eq. (1)]. Therefore, the discussion will be concerned first with the geometrical aspect through the variation of σ with the volume content of PANI, and then with the conductivity of the network through its temperature dependence.

a. Room-temperature conductivity versus volume content of PANI. A nonuniversal value of the exponent t has already been observed in blends containing conducting polymers. A value of t below 1.53 was reported in camphor sulfonic acid (CSA) doped PANI blends and attributed to hopping between disconnected parts of the conducting polymer network.[31,32] A case more similar to the present one with $t > 2$ was observed in polypyrrole/PEO blends.[33] To explain such a discrepancy with the predictions of the usual percolation model, more realistic percolation models can be invoked

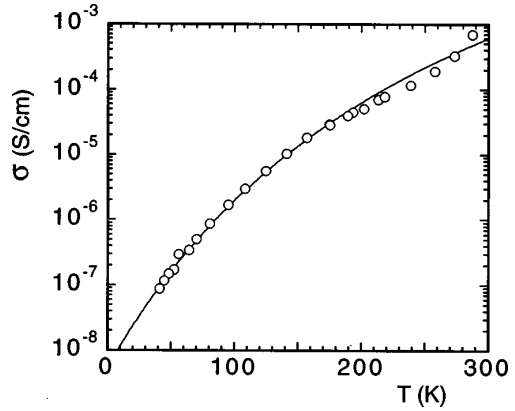

FIG. 10. Variation of σ vs T for the PANI/NAFION blend with 10 vol% PANI, and best fit obtained with Eq. (4).

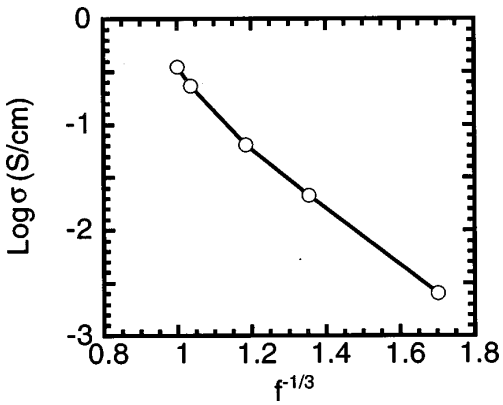

FIG. 11. $\ln(\sigma)$ vs $1/f^{1/3}$ for the PANI/POE blends, where f is the PANI volume content.

that take into account hopping and tunneling processes. In the classical model, two sites are considered to be connected when they are nearest neighbors. In this case the conductance between two sites depends neither on the distance nor on the energy levels of the sites and can only take the two extreme values 0 or 1. On the contrary, in the modified models, between sites one considers the possibility for hopping and tunneling processes through energetic barriers. This implies that the conductance between two sites is no longer of the binary type. We emphasize that such hopping processes prevail in bulk disordered conducting polymers. In the following it will be shown that it is actually the case in the conducting network of our PANI/PEO. Deviations from the universal scaling dependence are thus expected[34,35] and the material may conduct before continuous paths extending through the material are established. In the case of spherical particles in a polymer matrix, it was demonstrated through Monte Carlo simulations that t is increased above its theoretical value.[35] Moreover, the critical concentration f_c no longer means the formation of an infinite cluster of conducting particles in close contact but the formation of an infinite cluster for hopping conduction.

A particular type of such a model has been proposed by Ezquerra *et al.* for polypyrrole/PEO blends.[33] If the temperature is high enough so that the transition rates between two sites are mainly controlled by the distances between the sites, a linear dependence of $\ln(\sigma)$ versus $f^{-1/3}$ should be contained in the case of spherical particles. As shown in Fig. 11, such a law does not account very well for our data. This is probably due to the fact that the morphology of the PANI/PEO, as observed by SEM, has nothing to do with spherical particles of PANI embedded in the PEO matrix.

Finally, one should mention that deviations from the classical percolation problem are expected in the case of a mixture of good and bad conductors. It has been shown that the conductivity does not vanish at the percolation threshold,[29] and therefore that Eq. (1) is no longer valid. Doping heterogeneities in PANI/PEO blends revealed by UV VIS NIR spectroscopy could result in a distribution of the local conductivity of the PANI chains and therefore slightly contribute to the difference of the exponent t of Eq. (1) from its theoretical universal value.

Nevertheless, the percolation phenomenon most likely

controls the conductivity of PANI/PEO blends provided that hopping and tunneling processes are taken into account. Therefore, from a strict point of view, f_c cannot be considered as a percolation threshold. One should rather speak about a conductivity threshold which obviously is expected to occur at a lower volume content than the classic percolation one. Actually, f_c is located at around 4% in the PANI/PEO blends. While this value largely exceeds the very low ones (<1%) reported for CSA doped PANI-based blends,[31,32] it is clearly lower than the theoretical value of 16% for the percolation threshold in the case of globular conducting particles.[36] This rather low value is certainly an additional signature of the good interpenetration of the two polymers resulting in an entangled structure.

b. Temperature dependence of the conductivity. Let us now consider the temperature dependence of the conductivity and to the conduction mechanism that prevails in the conducting network of PANI. We stress the fact that the behavior described by Eq. (2b) may refer to several theoretical approaches that are based on very different microscopic pictures of the material. Among four models that lead to the same functional dependence, three are dealing with a homogeneous picture of the conducting material[37–39] while the fourth one is based on a heterogeneous picture.[14] This latter approach is the only one consistent with the UV visible spectroscopy data and the previous discussions that have shown that the PANI/PEO blends are actually heterogeneously doped. Besides, even in the case of bulk PANI, except for the highly conducting PANI protonated with surfactants like CSA, most of the data analysis of the electronic transport properties conclude in favor of a heterogeneous picture. Then, the same arguments used for ruling out the other models should lead to the same conclusion in the present discussion. However, one has to mention the model of hopping restricted to a homogeneous fractal sublattice,[38] of particular interest for the blends of conducting polymers. This model leads to an exponent $\alpha=3/7$ in Eq. (2a), which is very difficult to distinguish experimentally from $\alpha=1/2$. However, the different behavior of the conductivity expected at low temperature in this model is not experimentally observed.

Let us now consider the conducting islands model proposed by Zuppiroli *et al.*[14] for highly disordered conducting polymers, as an extension of the work of Sheng, Abeles, and Arie[40] on granular metals. This model has been successfully applied to various PANI blends[29] and to various conducting polymers like polypyrrole doped with polyelectrolytes involving tunneling effects through the dopant species.[14] It takes into account the disorder present in the polymer and the polaronic ground state characteristic of many conducting polymers rather than its quasi-one-dimensional structure. Conduction is supposed to proceed from hopping between small polaronic conducting grains separated by insulating barriers. The origin of such a heterogeneous structure could be in the nonuniform distribution of the counter-ions. In this model, the parameter T_0 [Eq. (2b)] is given by

$$T_0=\frac{8U}{k_B}\frac{s^2}{d^2}\frac{1}{1/2+s/d}, \tag{4}$$

where d is the average diameter of the conducting cluster, s the average distance between the clusters, and U the on-site Coulomb repulsion with an estimated value of about 4 eV.[41] The electronic transport through the sample is characterized by the charging energy between the conducting clusters, which is the electrostatic energy required to create a positive-negative charged pairs of grains. The model applies for cluster sizes small enough so that Ec is larger than the thermal energy kT.

In summary, this model takes into account both the heterogeneous structure revealed by the percolation phenomena and the doping heterogeneities inside the conducting pathway in the blends. Concerning the PANI/PEO blends, all the samples have a PANI volume fraction above the percolation threshold and transport occurs in a fully connected PANI pathway. But inside this pathway, there are doping heterogeneities and the conduction must be described with hopping. Since the doping level remains unchanged when the volume content of PANI is varied, the on-site Coulomb repulsion U can be regarded as constant with composition. In the framework of the model, the evolution of the parameter T_0 thus reflects changes in the geometry through the ratio s/d. This ratio increases from 0.13 to 0.35 when the PANI volume content is decreased from 100% to 20%. In other words, the fraction of highly conducting PANI in the conducting pathway shrinks when the PEO volume increases. This effect cannot be attributed to a change in the doping level.

2. PANI/NAFION

a. Room-temperature conductivity versus volume content of PANI. Contrary to the case of PANI/PEO, the room-temperature conductivity of PANI/NAFION is not a monotonous increasing function of the PANI volume content (see Fig. 7). Obviously, such a behavior cannot be accounted for by percolation models and one can wonder about the existence of any percolation threshold.

However, ac impedance spectroscopy measurements and a large improvement of the electroactivity combined with a disappearance of the resistive behavior in electrochemistry experiments above 10 vol% of PANI have strongly suggested that a percolation threshold actually exists, which takes place around 10 vol% of PANI.[13]

Until now, the fact that the doping level is changing with the composition of the blend has not been taken into account in the discussion. As already mentioned in the framework of percolation theory, the geometrical aspect of the conducting network is responsible for the scaling term in Eq. (1), while the intrinsic conductivity of the material constituting this network appears in the C term of Eq. (1). It is therefore very tempting to normalize the conductivity of each sample with respect to that of the bulk PANI having the same doping level. From the variation of the conductivity in PANI as a function of the doping level,[42] we have taken the following values: $\sigma_{\mathrm{PANI}}(40\%)=1$ S/cm, $\sigma_{\mathrm{PANI}}(30\%)=0.1$ S/cm, $\sigma_{\mathrm{PANI}}(20\%)=5.10^{-4}$ S/cm. The normalized conductivity $RA(f)=\sigma(f)/\sigma_{\mathrm{PANI}}(f)$, where $\sigma(f)$ is the room-temperature conductivity of the blend and $\sigma_{\mathrm{PANI}}(f)$ the conductivity of pure PANI for the corresponding doping level, is plotted in Fig. 12 on a logarithmic scale versus the volume content of PANI. As one can see, the variation of RA looks like that expected in a percolation phenomenon. Thus, the conductiv-

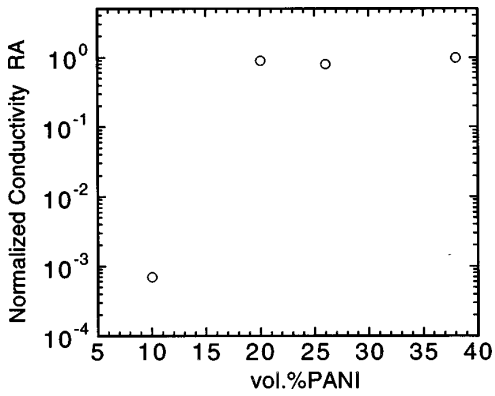

FIG. 12. Variation of the ratio, RA, of the room-temperature conductivity σ of the PANI/NAFION blend to the conductivity of pure PANI, σ_{PANI}, for the corresponding doping level, as a function of the volume content of PANI (see text).

ity of the PANI/NAFION blends can be qualitatively described by the relation

$$\sigma \propto \sigma_{\mathrm{PANI}}(f)(f-f_c)^t, \tag{5}$$

where $\sigma_{\mathrm{PANI}}(f)$ represents the conductivity of the percolating material, which is indirectly dependent on the volume content of PANI through the doping level. The best fit leads to $10\% < f_c < 15\%$. The opposite variation of $\sigma_{\mathrm{PANI}}(f)$ and $(f-f_c)^t$ as a function of the PANI volume content f leads to the experimental bell-shaped curve given in Fig. 7.

From the above analysis, it appears that all the blends are characterized by a fully connected pathway including doping heterogeneities except the one with 10 vol% of PANI. Despite its higher doping level, the latter blend is considerably less conducting than the 20 vol% one because it is just below the percolation threshold.

b. Temperature dependence of the conductivity above the percolation threshold. In contrast to PEO in the PANI/PEO, the Nafion ionomer acts both as an insulating polymer and as a counterion in the doping process. The conducting pathway should thus necessarily be made up of a mixture of NAFION and PANI. It should correspond to the connected dark domains observed with TEM. Inside this pathway, the thermal variation law of the conductivity, $\sigma(T) = \sigma_0 \exp[-(T_0/T)^{1/2}]$, strongly suggests that the transport process is governed by doping heterogeneities that may have been generated by topological constraints on the ionomer (Fig. 8). In the highly conducting regions, the sulfonated groups of NAFION are likely to act as dopants and therefore as bridges between the PANI chains, thus enhancing the interchain transfer. On the contrary, in the clear regions of the TEM pictures of Fig. 3(a) the pure phase of the ionomer could constitute an insulating barrier. To proceed further with the interpretation of the data, we have to discuss the variation of T_0 with the PANI volume content in the framework of the conducting islands model.[14] The on-site Coulomb repulsion U can no longer be definitely regarded as constant since the doping level varies with the composition. One could expect that electrostatic interactions are, to a certain extent, less screened and that U is increased when the doping level, and thus the conductivity, are decreased. Therefore, the slight decrease of T_0, from 4.4×10^{4}K to 2.2×10^{4} K for decreasing PANI volume contents, cannot be exclusively attributed to a decrease of the ratio s/d and accordingly to an increase of the volume fraction of highly conducting regions inside the conducting pathway.

c. Temperature dependence of the conductivity below the percolation threshold. As regards the specific case of the blend with 10 vol% PANI, we are dealing with the FIT type of variation of the conductivity, $\sigma(T) = \sigma_0 \exp[-T_1/(T+T_0)]$. Such a dependence has already been observed in highly conducting polymers and in PVC-carbon composites.[30,43–46] But here the point is that the conductivity of the blend is significantly lower than the ones reported in this work.

The FIT-type dependence prevails in heterogeneous systems where large conducting regions are separated by thin insulating barriers. When the average diameter of the conducting islands is large enough, the charging energy becomes negligible as compared to the thermal energy. Thus, the conductivity is only limited by the probability of the charge carriers to hop over or through the barriers. At this point, two mechanisms may be considered that lead to the same temperature dependence of the conductivity as given by Eq. (3). On the one hand, the FIT model of Sheng says that the voltage across the barriers may be subject to large thermal fluctuations leading to a modulation of the tunneling probability. The analysis of T_0 and T_1 based on the simple relations derived by Paasch, Lehman, and Wuckel[44] yields unrealistic values for the width and the mean area of the barrier. On the other hand, Schimmel *et al.*[46] proposed a phenomenological model that can account for the same variation law. At low temperature, hopping occurs via tunneling through the barriers, while thermal activation over the potential barrier dominates at high temperature. Within this approach, the height of the barrier is given by

$$\Delta E = k_B T_1, \tag{6}$$

while its width s is related to T_0 and $T_1$by

$$\frac{T_1}{T_0} = \sqrt{2m\Delta E}\frac{2s}{\hbar}. \tag{7}$$

In the framework of this approach, the analysis leads to $s \approx 25$ Å and $\Delta E \approx 0.5$ eV, which are reasonable values. The numerical values of T_1 and T_0 are usually much lower in bulk conducting polymers and thus the corresponding barriers are much lower. As pointed out by Sheng[30] and Paasch *et al.*,[44] the consistency of the Schimmel model and the domination of thermal activation mechanism requires large junction areas in which the barrier height is not significantly reduced by thermal fluctuations. This condition can be easily fulfilled by considering large conducting grains, which are likely to be present in this blend as explained above.

In the particular blend that is located just below the percolation threshold, the conducting pathway made up of PANI and NAFION is expected to be disconnected. Nevertheless, most of this interrupted conducting pathway is made up of highly conducting regions. The high doping level in this

sample is associated with rather large but disconnected conducting islands. The junctions between these clusters are very large too.

IV. CONCLUSION

In the present work, the electronic transport processes in PANI/PEO and PANI/NAFION blends have been studied in relationship to the organization of the PANI phase and the PANI protonation levels.

The doping levels of PANI have been determined from elemental analysis and XPS measurements. Despite the liquid phase protonation of the emeraldine base chains, spectroscopic measurements have shown that doping heterogeneities are still present in PANI. Concerning the PANI/PEO blends, the average doping level of PANI does not depend on the composition. We have shown that the percolation theory can describe the variation of the room-temperature conductivity with the PANI volume content provided that hopping and tunneling processes and doping heterogeneities are taken into account. The transport process can be explained in the framework of a hopping model between highly conducting clusters embedded in the PANI fully connected pathway. An increase of the PEO concentration results in a decrease of the fraction of the highly conducting regions inside the PANI pathway.

In the PANI/NAFION blends, the situation is quite different. While the volume content of PANI is increased, it appears that (i) the average doping level of PANI decreases, and (ii) the conductivity goes through a maximum and then decreases. We have shown that the maximum results from the competition between two opposite effects of the composition on the conductivity of the blend: (i) an increase due to the scaling law of classical percolation theory, and (ii) a decrease coming from the decreasing intrinsic conductivity of the percolation network induced by a lower and lower doping level.

As in PANI/PEO, the conduction mechanism that prevails in most of the PANI/NAFION blends (20, 26, and 38% of PANI) has been shown to rely on hopping processes between highly conducting regions inside a PANI connected pathway. A different behavior has been shown in the 10% PANI volume content sample. The temperature dependence of the conductivity can be accounted for by the fluctuation-induced tunneling mechanism, which corresponds to a disconnected pathway between very large conducting grains in agreement with the fact that this particular composition is below the percolation threshold. Such a large grain size may be attributed to the high doping level reached for this composition. This strongly suggests that the fraction of highly conducting PANI regions in PANI/NAFION is an increasing function, not of the PANI concentration as in PANI/POE, but of the doping level reached for a given composition.

---

*Member of the CNRS.

[1] A. Fizazi, J. Moulton, K. Pakbaz, S. D. Rughooputh, P. Smith, and A. J. Heeger, Phys. Rev. Lett. **64**, 2180 (1990).

[2] Y. Y. Suzuki, A. J. Heeger, and P. Pincus, Macromolecules **23**, 4730 (1990).

[3] A. Andreatta, A. J. Heeger, and P. Smith, Polym. Commun. **31**, 275 (1990).

[4] Y. Wang and M. F. Rubner, Macromolecules **25**, 3284 (1992).

[5] M. Makhlouki, M. Morsli, A. Bonnet, A. Conan, A. Pron, and S. Lefrant, J. Appl. Polym. Sci. **44**, 443 (1992).

[6] C. K. Subramaniam, A. B. Kaiser, P. W. Gilberd, and B. WeBling, J. Polym. Sci. B **31**, 1425 (1993).

[7] R. Pelster, G. Nimtz, and B. Wessling, Phys. Rev. B **49**, 12 718 (1994).

[8] Y. Cao, P. Smith, and A. J. Heeger, Synth. Met. **48**, 91 (1992).

[9] C. Y. Yang, Y. Cao, P. Smith, and A. J. Heeger, Synth. Met. **53**, 293 (1993).

[10] M. Reghu, C. O. Yoon, C. Y. Yang, D. Moses, A. J. Heeger, and Y. Cao, Macromolecules **26**, 7245 (1993).

[11] C. O. Yoon, M. Reghu, D. Moses, A. J. Heeger, and Y. Cao, Phys. Rev. B **48**, 14 080 (1993).

[12] D. Orata and D. A. Buttry, J. Electroanal. Chem. **257**, 71 (1988); P. Aldebert, P. Audebert, M. Armand, G. Bidan, and M. Pineri, J. Chem. Soc. Chem. Commun. **22**, 1636 (1986).

[13] C. Barthet and M. Guglielmi, Electrochim. Acta **41**, 2791 (1996).

[14] L. Zuppiroli, M. N. Bussac, S. Paschen, O. Chauvet, and L. Forro, Phys. Rev. B **50**, 5196 (1994).

[15] L. S. Yang, Z. Q. Shan, and Y. D. Liu, Solid State Ion. **40-41**, 967 (1990); W. Baochen, F. Li, and X. Yongyao, J. Power Sources **43-44**, 83 (1993).

[16] M. Morita, R. Miyake, H. Tsutsumi, and Y. Matsuda, Chem. Express **5**, 985 (1990).

[17] C. S. C. Bose, S. Basak, and K. Rajeshwar, J. Electrochem. Soc. **75**, 139 (1992).

[18] J. Y. Sung and H. J. Huang, Anal. Chim. Acta **246**, 275 (1991).

[19] T. Hirai, S. Kuwabata, and H. Yoneyama, J. Electrochem. Soc. **135**, 1132 (1988).

[20] M. Angelopoulos, C. E. Asturier, S. P. Erme, E. Ray, E. M. Scherr, A. G. MacDiarmid, M. A. Aktar, Z. Kiss, and A. J. Epstein, Mol. Cryst. Liq. Cryst. **160**, 151 (1988).

[21] C. Barthet, thesis UJF Grenoble, 1995.

[22] C. Barthet and M. Guglielmi (unpublished).

[23] Janssen Catalog.

[24] C. Barthet and M. Guglielmi, J. Electroanal. Chem. **388**, 35 (1995).

[25] A. J. Epstein, J. M. Ginder, F. Zuo, R. W. Bigelow, H. S. Woo, D. B. Tanner, A. F. Richter, W. S. Huang, and A. G. MacDiarmid, Synth. Met. **18**, 303 (1987).

[26] K. G. Neoh, E. T. Kang, and K. L. Tan, Polymer **33**, 2292 (1992); C. B. Duke, E. M. Conwell, and A. Paton, Chem. Phys. Lett. **131**, 82 (1986).

[27] D. Stauffer, *Introduction to Percolation Theory* (Taylor and Francis, London, 1985); D. Stauffer, Phys. Rep. **54**, 1 (1985); J. P. Clerc, G. Giraud, and J. M. Luck, Adv. Phys. **39**, 191 (1990); D. J. Bergman and D. Stroud, Solid State Phys. **46**, 147 (1992).

[28] V. Van der Putten, J. T. Moonen, B. Brom, J. C. M. Brokken-Zijp, and M. A. Michels, Phys. Rev. Lett. **69**, 494 (1992).

[29] F. Zuo, M. Angelopoulos, A. G. MacDiarmid, and A. J. Epstein, Phys. Rev. B **36**, 3475 (1987); M. Wan, M. Li, J. Li, and Z. Liu, Thin Solid Films **259**, 188 (1995); R. Pelster, G. Nimtz, and B. Wessling, Phys. Rev. B **49**, 12 718 (1994); F. Lux, G. Hinrichsen, V. I. Krinichnyi, I. B. Nazarova, S. D. Cheremisov, and M. M. Pohl, Synth. Met. **55-57**, 347 (1993); A. B. Kaiser, C. K. Subramaniam, P. W. Gilberd, and B. Wessling, *ibid*. **69**, 197 (1994).

[30] P. Sheng, Phys. Rev. B **21**, 2180 (1980).
[31] M. Reghu, C. O. Yoon, C. Y. Yang, D. Moses, P. Smith, and A. J. Heeger, Phys. Rev. B **50**, 13 931 (1994).
[32] C. O. Yoon, M. Reghu, D. Moses, A. J. Heeger, and Y. Cao, Synth. Met. **63**, 47 (1994).
[33] T. A. Ezquerra, M. Mohamadi, F. Kremer, T. Vilgis, and G. Wegner, J. Phys. C **21**, 927 (1988).
[34] A. K. Sarychev and F. Brouers, Phys. Rev. Lett. **73**, 2895 (1994).
[35] I. A. Tchmutin, A. T. Ponomarenlo, V. G. Shevehenko, and D. Y. Godovski, Synth. Met. **66**, 19 (1994).
[36] R. Zallen, *The Physics of Amorphous Solids* (Wiley, New York, 1983).
[37] E. P. Nakhmedov, V. N. Prigodin, and A. N. Samukhin, Fiz. Tverd. Tela (Leningrad) **31**, 31 (1989) [Sov. Phys. Solid State **31**, 368 (1989)]; Z. H. Wang, A. Ray, A. G. MacDiarmid, and A. J. Epstein, Phys. Rev. B **43**, 4373 (1991).
[38] G. Deutscher, Y. Levy, and B. Souillard, Europhys. Lett. **4**, 577 (1989); A. Aharony, O. Entin-Wohlman, and A. B. Harris, Physica A **200**, 171 (1993); A. Aharony, A. B. Harris, and O. Entin-Wohlman, Phys. Rev. Lett. **70**, 4160 (1993).
[39] A. L. Efros and B. J. Shklovskii, J. Phys. C **8**, L49 (1975).
[40] P. Sheng, B. Abeles, and Y. Arie, Phys. Rev. Lett. **31**, 44 (1973).
[41] M. N. Bussac and L. Zuppiroli, Phys. Rev. B **47**, 5493 (1993).
[42] A. G. MacDiarmid, J. C. Chiang, and A. G. Richter, Synth. Met. **18**, 285 (1987).
[43] R. Mertens, P. Nagels, R. Callaerts, J. Briers, and H. J. Geise, Synth. Met. **55-57**, 3538 (1993).
[44] G. Paasch, G. Lehmann, and L. Wuckel, Synth. Met. **37**, 23 (1990).
[45] J. Voit and H. Büttner, Solid State Commun. **67**, 1233 (1988).
[46] T. Schimmel, G. Denninger, W. Riess, J. Voit, M. Schoerer, W. Schoepe, and H. Naarman, Synth. Met. **28**, 11 (1989).